Uniaxial and tensile strained germanium nanomembranes in rolled-up geometry by polarized Raman scattering spectroscopy

Qinglei Guo, Miao Zhang, Zhongying Xue, Jing Zhang, Gang Wang, Da Chen, Zhiqiang Mu, Gaoshan Huang, Yongfeng Mei, Zengfeng Di, and Xi Wang

Citation: AIP Advances **5**, 037115 (2015); doi: 10.1063/1.4914916

View online: https://doi.org/10.1063/1.4914916

View Table of Contents: http://aip.scitation.org/toc/adv/5/3

Published by the American Institute of Physics

AIP ADVANCES **5**, 037115 (2015)

Uniaxial and tensile strained germanium nanomembranes in rolled-up geometry by polarized Raman scattering spectroscopy

Qinglei Guo,[1] Miao Zhang,[1] Zhongying Xue,[1] Jing Zhang,[2] Gang Wang,[1] Da Chen,[1] Zhiqiang Mu,[1] Gaoshan Huang,[2] Yongfeng Mei,[2,a] Zengfeng Di,[1,a] and Xi Wang[1]

[1]*State Key Laboratory of Functional Materials for Informatics, Shanghai Institute of Microsystem and Information Technology, Chinese Academy of Sciences, 865 Changning Road, Shanghai 200050, People's Republic of China*

[2]*Department of Materials Science, Fudan University, Shanghai 200433, People's Republic of China*

(Received 26 January 2015; accepted 3 March 2015; published online 10 March 2015)

We present a rolled-up approach to form Ge microtubes and their array by rolling-up hybrid Ge/Cr nanomembranes, which is driven by the built-in stress in the deposited Cr layer. The study of Raman intensity as a function of the angle between the crystal-axis and the polarization-direction of the scattered light, i.e., polarized Raman measurement reveals that the strain state in Ge tube is uniaxial and tensile, and can reach a maximal value 1.0%. Both experimental observations and theoretical calculations suggest that the uniaxial-tensile strain residual in the rolled-up Ge tubes correlates with their tube diameters, which can be tuned by the thicknesses of the Cr layers deposited. Using the polarized Raman scattering spectroscopy, our study provides a comprehensive analysis of the strain state and evolution in self-rolled-up nano/micro-tubes. [http://dx.doi.org/10.1063/1.4914916]

Due to their unique geometries and distinct physical properties, micro/nanotubes have been explored in the application of biology,[1] optics,[2] electronics,[3] and mechanics.[4] Roll-up nanotechnology has been proven as a convenient approach to fabricate micro/nanotubes, as reported previously.[5–9] By releasing the built-in mechanical stress, the rolling-up process induces the curving of the original flat films, thus resulting in the change of their strain status[10] in the rolled-up geometry[11] (SiGe/Si tubes or III-V tubes), which have been confirmed by micro-Raman scattering,[12] X-ray microdiffractions,[10,13,14] and photoluminescence spectroscopy.[15] Meanwhile, physical properties of semiconductor nanomembranes (NMs),[16,17] such as band structures,[18,19] and carrier mobilities,[20] could be altered by the intrinsic strain/stress.[21] As integrated circuit technology is entering 22nm node, strain is still employed to boost the carrier mobility in the channel of Si-based metal oxide semiconductor field effect transistors (MOSFETs). Other than the mobility enhancement, strain-engineering is also promising to improve the direct-transition optical gain of Ge due to its particular band structure.[22] To be the most promising candidate to replace Si as the microelectronic and optoelectronic technologies enter post-Si era, tensile-strained Ge has been exploited and fabricated by various external mechanical stress approaches, such as mechanically stretched by high-pressure gas,[23,24] three-point straining platform,[25] Si_3N_4 stressor layers,[18] or strain concentrating in microbridges.[19]

In this letter, we present a combined and convenient approach to introduce strain into Ge NMs by rolled-up process, and the strain state and evolution is investigated by the polarized micro-Raman scattering spectroscopy. The rolling-up process consists of patterning and under-etching the constricted buried oxide (BOX) from Cr/Germanium-on-insulator (GOI) structure. Due to the

[a]Corresponding author: Prof. Yongfeng Mei Email: yfm@fudan.edu.cn. Prof. Zengfeng Di Email: zfdi@mail.sim.ac.cn.

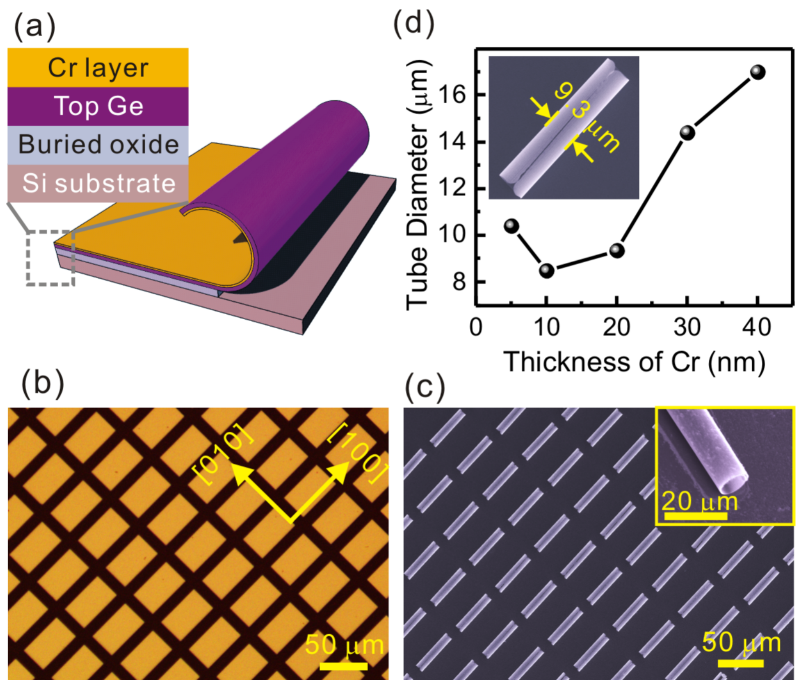

FIG. 1. (a) Schematic diagram illustrating the rolling-up process of the hybrid Ge/Cr nanomembranes into a tube. (b) Optical microscopy image of the unreleased GOI (as-patterned GOI wafer). (c) SEM image of the released Ge tube array. (d) Ge tube diameter as a function of the thickness of Cr layer deposited.

built-in stress in Cr films, the Cr/Ge bilayer structure rolls up automatically into a tube configuration, thus generating the tensile strain in the formed Ge tubes. The polarized Raman scattering spectroscopy as a function of the angle between the crystal-axis and the polarization-direction of the scattered-light indicates the generated tensile strain is uniaxial. The hyperspectral Raman measurements together with the calculation results demonstrate that the uniaxial-tensile strain in the rolled-up Ge tubes varies with the diameter of Ge tubes, which can be tuned by the thickness of the Cr layer deposited.

The schematic illustration of the rolled-up Ge tubes fabricated with strain-released Ge/Cr NMs is presented in FIG. 1(a). First, a photoresist (AZ 5214) was spin-coated and patterned into rectangles ($30 \times 50\ \mu m^2$) on a (100) GOI wafer with a 50 nm-thick Ge NMs, and the long sides of the rectangles were designed to be parallel to [100] direction of the top Ge layer. Subsequently, Cr layers with different thicknesses were deposited at a constant rate of 2 Å/s by e-beam evaporation. It should be noted that the growth condition for Cr layer was tuned to achieve the adequate built-in stress for the subsequent Ge tubes formation. After the lift-off process, the Cr film was patterned into the array of Cr rectangles. Then, the Cr rectangle array was used as a mask to transfer the pattern to the Ge NMs of GOI wafer by reactive ion etching using SF_6 and O_2. The optical image of the array is shown in FIG. 1(b). As the obtained pattern structure was immersed into HF solution, the BOX of GOI substrate was selectively etched, and then the hybrid Ge/Cr layer stacks were released and detached from the substrate. Driven by the built-in tensile stress in the top Cr NM,[26] the Ge/Cr NMs rolled up and formed the tube structure, as displayed FIG. 1(c). As reported previously, the rolling-up direction is mainly determined by the geometry of the released pattern,[27] and the Young's modulus of the released material.[28] For the Ge/Cr rectangle pattern with the geometry particularly designed, it also rolls up from the long side [FIG. 1(c)]. Meanwhile, the rolling direction of the tube is also along <100> direction where Young's modulus is small.[28] It is further observed that the diameter of the Ge tube can be tuned by varying the thickness of the Cr layer as shown in FIG. 1(d). For the typical hybrid Ge/Cr (50 nm/20 nm) NM stacks, the diameter of the Ge tube is ~9.3 μm, as exhibited in the insert of FIG. 1(d).

Micro-Raman spectroscopy has been routinely applied to analyze the strain distribution of semiconductor films.[12] However, recent studies suggest the strain-induced Raman shifts of suspended nanostructures are always entangled with the local laser heating effect, thus leading to the overestimation (underestimation) of the tensile (compressive) strain.[29,30] In term of the thermal dissipation, the unique tube structure is expected to be even worse than the suspended nanostructure, since the micro cavity surrounded by the sidewall of tubes can further retard the thermal dissipation. Therefore, to accurately identify the strain-induced Raman shifts in the Ge tubes, the local laser heating effect should be considered systematically. Micro-Raman spectra of the unreleased GOI wafer and released tubes [FIG. 1(c)] are recorded with the varying excitation laser (laser spot: ~1 μmϕ; wavelength: 325 nm) power, as displayed in FIG. 2(a). The power-dependent peak positions for Ge-Ge vibration mode obtained from unreleased GOI wafer and released Ge tubes are summarized in Fig. 2(b). For the

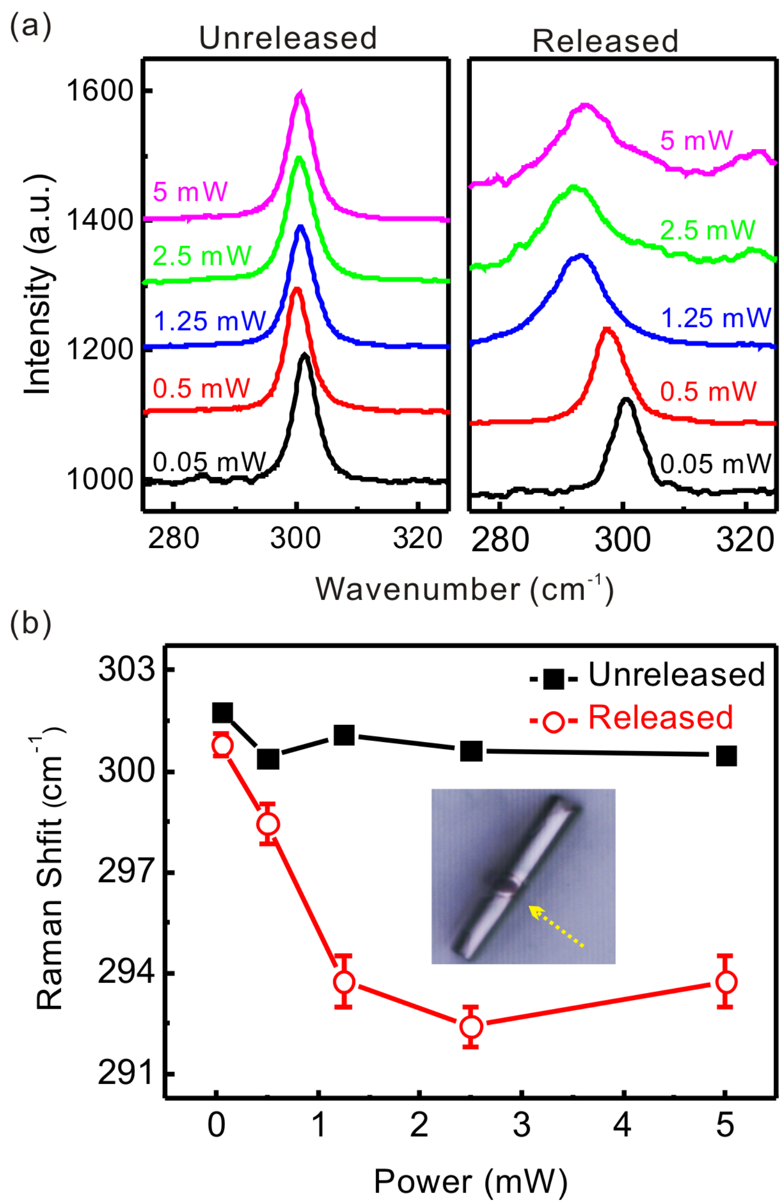

FIG. 2. (a) Power-dependent Raman spectra of unreleased GOI (left) and released Ge tube (right). (b) Peak positions for unreleased GOI and released Ge tube as a function of the power of excitation laser. The insert shows a typical optical microscopy image of a burnt-out released Ge tube, which is subject to the excitation laser with the power over 1.25 mW.

unreleased GOI wafer, the Ge-Ge peak position only has slight variations as the power of excitation laser changes from 0.05 to 5 mW, which suggests the adequate thermal dissipation.[29] However, for the released Ge tube, the Ge-Ge peak position shifts to the low wavenumber monotonically as the power of excitation laser increases from 0.05 to 1.25 mW. When the excitation laser power approaches 1.25 mW or above, the local laser heating effect becomes rather severe and overwhelming, thus leading to the ruins of Ge tubes, as highlighted by the arrow in the insert of FIG. 2(b). As demonstrated in FIG. 2(b), the Raman shift obtained by the laser with 0.05 mW power is close to the virtual one using zero laser power,[29] therefore the laser power of 0.05mW is selected for the following Raman characterization.

Since the polarized Raman scattering intensities closely correlate to the crystal orientation,[31] micro-Raman scattering measurements under polarization filtering of the scattered-light can be further employed to distinguish the uni- or bi-axial strains.[31,32] In this study, the polarized Raman scattering spectroscopy as a function of the angle between the crystal-axis and the polarization-direction of the scattered-light is performed on the released Ge tubes to determine its strain state. Schematic setup of polarized Raman scattering measurement is displayed in Fig. 3(a). The polarization vector of the excitation laser is expressed as e_i, and the angle between e_i and [100] direction is denoted as θ which can be changed by rotating the released Ge tube (sketched) or the unreleased GOI wafer (not shown). A schematic diagram of three lattice-parameter components from a released Ge tube: radial (a_r), tangential (a_t) and longitudinal (a_l) is also shown in the inset of

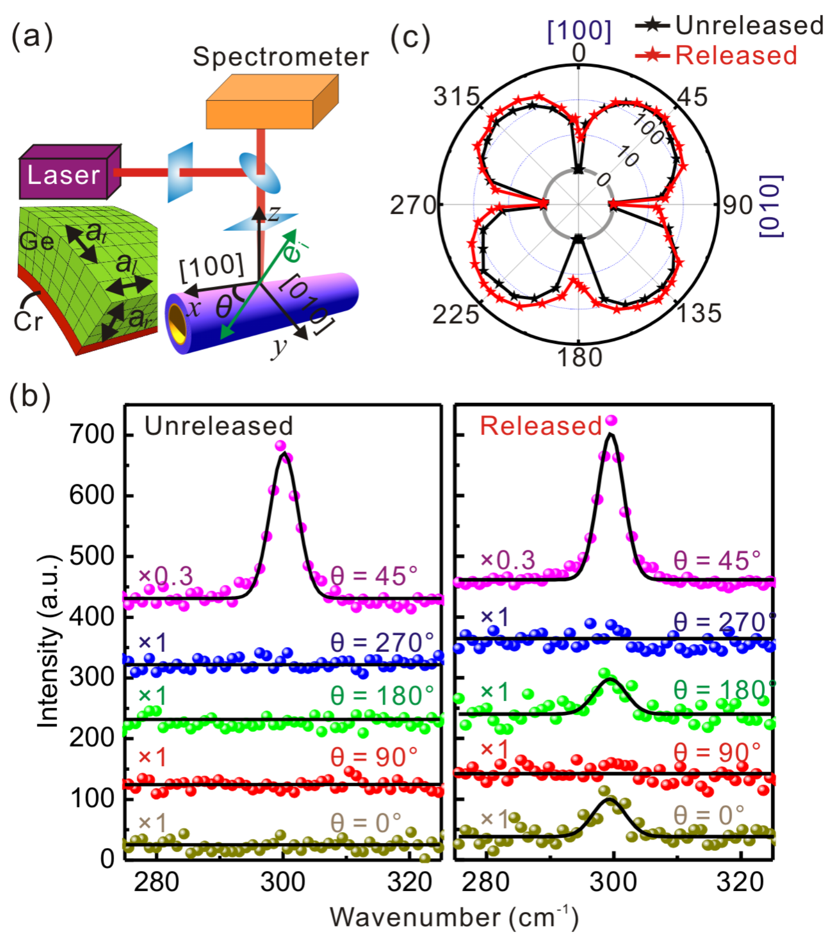

FIG. 3. (a) Schematics of the polarized Raman scattering measurement on released Ge tube and three lattice-parameter components from a roll-up tube. (b) Typical polarized Raman spectra obtained from unreleased GOI wafer (left) and released Ge tube (right). The black lines represent the corresponding Lorentz fitting of the spectra. (c) The θ-dependent of the polarized Raman peak intensities for Ge-Ge vibration mode obtained from unreleased GOI and released Ge tube.

FIG. 3(a). Figure 3(b) displays the typical polarized Raman spectra obtained from the unreleased GOI wafer and the released Ge tube. For the unreleased GOI wafer, the Raman scattering signals observed at $\theta = 45°$ present the characteristic Ge-Ge vibration mode located at $\sim$301 cm^{-1} which vanishes away at $\theta = 0°$, $\theta = 90°$, $\theta = 180°$ and $\theta = 270°$. The θ-dependent of the intensities for Ge-Ge vibration mode measured on unreleased GOI wafer is summarized in Fig. 3(c), which clearly indicates a 90° periodicity. For cubic crystal, e.g., strain-free Si, the polarized Raman scattering becomes inactive along [100] and [010] direction, thus leading to 90° periodicity, as reported by Mizoguchi *et al*. and Kurosawa *et al*.[31,32] Therefore, similar to bulk Si, the starting Ge NMs of unreleased GOI wafer also possess the symmetric cubic structure, and no strain is present.

For the released Ge tube, since the rolling direction of the hybrid Ge/Cr layers is along [010] direction, as shown in Fig. 3(a), strain can be generated along the rolled-up direction according to the bending effect.[33] In Fig. 3(b), polarized Raman results obtained from the released Ge tube exhibit the most prominent Ge-Ge vibration peak at $\theta = 45°$. The intensity of Ge-Ge vibration peak decreases but essentially exists at $\theta = 0°$ and $\theta = 180°$, while totally disappears at $\theta = 90°$ and $\theta = 270°$. The θ-dependent of the intensities for Ge-Ge vibration mode is summarized in Fig. 3(c), which clearly indicates a 180° periodicity. Considering the schematic setup of polarized Raman scattering system in Fig. 3(a), the Ge-Ge vibration mode of the released Ge tube is inactive when the polarization vector of the excitation laser along [010], and becomes active along [100]. Compared to the unreleased GOI wafer, the results obtained from the released Ge tube suggest the polarized Raman peak at $\theta = 0°$ and $\theta = 180°$, which is inactive for strain-free unreleased GOI wafer, becomes active under the stress field induced along [010] direction. Therefore, the strain in Ge tube originating from the rolling-up process is uniaxial, which induces the asymmetric-change in cubic crystal structure. The asymmetric crystal structure of the rolled-up Ge tube results in the modification of the selection-rule for the polarized Raman scattering spectroscopy.[32] Since the uniaxial-tensile strain only distributes along the rolling direction of Ge tube, the lattice parameter a_t of the Ge tube along the rolling direction is expanded, while a_l along the longitudinal direction [FIG. 3(a)] could not be influenced and keep the same as that of the unreleased GOI.

Finally, hyperspectral Raman measurements on released Ge tubes with different diameters [shown in FIG. 1(c)] are performed, and the spectral resolution is 0.1 cm^{-1}. The dimension-dependent peak positions for Ge-Ge vibration modes of the released Ge tubes are summarized in FIG. 4(a), and that of unreleased GOI wafer is plotted for reference (dashed gray line). The Ge-Ge mode peaks measured on released Ge tubes display distinctly down-shifts with respect to the unreleased GOI wafer, indicating the presence of tensile strain created by the rolling-up process. By considering the influence from the phonon deformation potentials,[31] the relation between Raman shifts and the tangential strain ε_{yy} in uniaxial-strained Ge tube, i.e., [010] in FIG. 3(a), is expressed by[25]

$$\Delta\omega_{\mathrm{bulk}} = -k \times \varepsilon_{yy} \tag{1}$$

Where $\Delta\omega_{\mathrm{bulk}}$ represents the relative shift of the peak position of Ge-Ge vibration mode between released Ge tubes and unreleased GOI, i.e., $\omega_{\mathrm{strained}} - \omega_{\mathrm{bulk}}$. $k = 0.646$ denotes a proportionality factor for uniaxial-strained Ge.[19] According to Eq. (1), the deduced uniaxial strain values of the released Ge tubes with various diameters are summarized in FIG. 4(b). As the diameter of the released tubes decreases to around 8μm, the consequent uniaxial strain increases up to ~1%. The generation of uniaxial strain by the rolling-up process is also analyzed by the theoretical calculation. The rolling-up process can been considered as the bending the hybrid Ge/Cr layers to extremely small radii. The strain, ε, in the released Ge tubes can be calculated by the following equation[33]

$$\varepsilon = \frac{(\mathrm{d_{Ge}} + \mathrm{d_{Cr}})}{2\mathrm{r}} \frac{(1 + 2\eta + \chi\eta^2)}{(1 + \eta)(1 + \chi\eta)}, \tag{2}$$

where $\mathrm{d_{Ge}}$ and $\mathrm{d_{Cr}}$ are the layer thicknesses for the top Ge NM of GOI and as-deposited Cr layer, respectively. r is the radius of the released Ge tubes. $\eta = \mathrm{d_{Cr}}/\mathrm{d_{Ge}}$ and $\chi = Y_{\mathrm{Cr}}/Y_{\mathrm{Ge}}$, where Y_{Ge} and Y_{cr} are the elastic Young's moduli for the Ge NM and the Cr layer, respectively. Based on Eq. (2), the calculated strain values for the released Ge tubes with different diameters are also displayed in

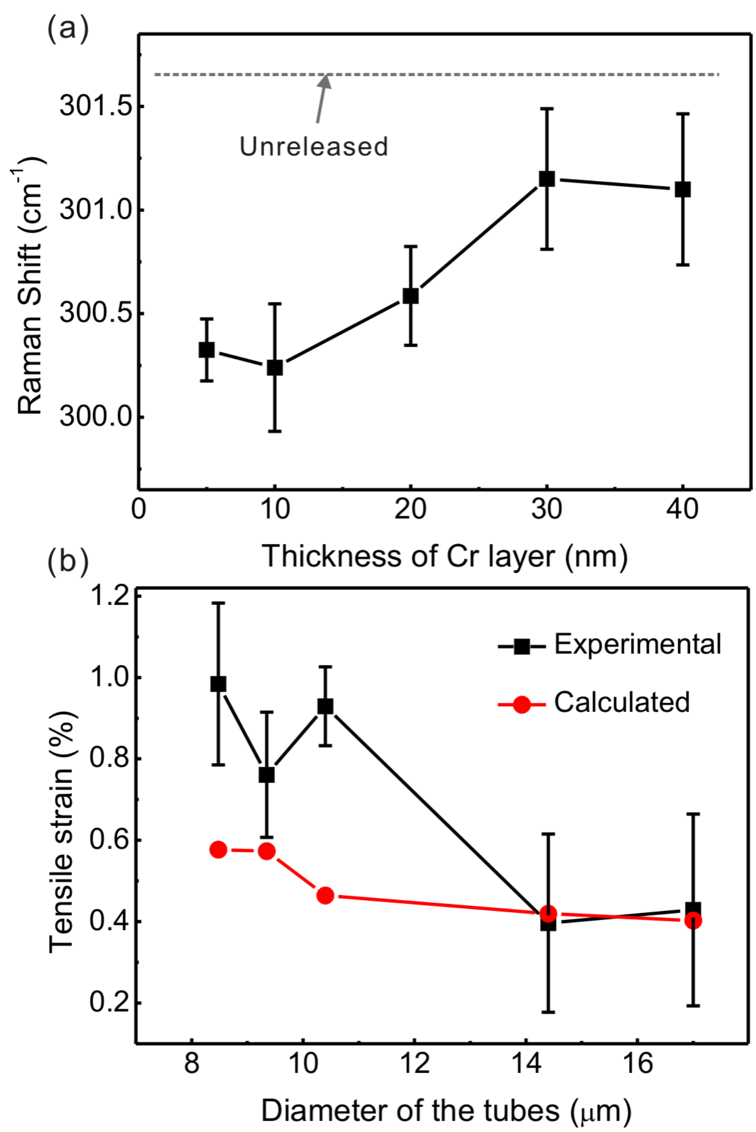

FIG. 4. (a) Raman peak position obtained from released Ge tubes and unreleased GOI (dashed line) under the power of the excitation laser 0.05 mW. (b) Experimental and calculated strain values of Ge tubes with different diameters.

FIG. 4(b) as well. It is found that the calculated values fairly agree with the experimental observations. The minor discrepancy between experiment measurements and theoretical calculations is assumed to be due to two possible reasons: (i) the reduced but unavoidable thermal effect on released tubes by local laser heating;[29] (ii) the strain variation along the side-wall of the tubes and z direction.[34] As shown in FIG. 2, the laser-heating effect, though greatly suppressed to the utmost, can cause the shift of Raman peak of the Ge-Ge mode towards lower wavenumber, thus resulting in the overestimation of the strain value. Furthermore, the focusing of the excitation laser on the circular Ge tubes is extremely difficult; therefore, the contribution from the side-wall or the deep region other than the top surface of Ge tube may induce the perturbation of the obtained strain value as well.

In summary, the Ge tube array has been achieved by roll-up nanotechnology, and the diameters of Ge tubes are tuned by the thickness of Cr layer in the hybrid Ge/Cr nanomembranes. With the minimization of the laser heating effect, the strain existing in the tubes has been systematically studied by polarized Raman scattering and hyperspectral Raman measurements. The obtained

θ-dependent polarized Raman scattering intensities ensure that the strain state of the rolled-up Ge tubes is uniaxial. Both the calculation results and the experimental data suggest the uniaxial-tensile strain residual in the rolled-up Ge tubes correlates with the diameter of Ge tube, which is controlled by the thickness of Cr layer with built-in stress.

ACKNOWLEDGMENT

This work was financially supported by Creative Research Groups of National Natural Science Foundation of China (No. 61321492), National Natural Science Foundation of China under Grant Nos. 61176001, 51222211, 61274136, & 51322201, Specialized Research Fund for the Doctoral Program of Higher Education (No. 20120071110025), Science and Technology Commission of Shanghai Municipality (14JC1400200), Chinese Academy of Sciences (CAS) International Collaboration and Innovation Program on High Mobility Materials Engineering, and One Hundred Talent project from CAS.

[1] G. S. Huang, Y. F. Mei, D. J. Thurmer, E. Coric, and O. G. Schmidt, Lab Chip **9**, 263 (2009).
[2] G. S. Huang, V. A. Bolanos Quinones, F. Ding, S. Kiravittaya, Y. F. Mei, and O. G. Schmidt, ACS Nano **4**, 3123 (2010).
[3] C. C. Bof Bufon, J. D. Arias Espinoza, D. J. Thurmer, M. Bauer, Ch. Deneke, U. Zschieschang, H. Klauk, and O. G. Schmidt, Nano Lett. **11**, 3727 (2011).
[4] Y. F. Mei, A. A. Solovev, S. Sanchez, and O. G. Schmidt, Chem. Soc. Rev. **40**, 2109 (2011).
[5] V. Y. Prinz, V. A. Seleznev, A. K. Gutakovsky, A. V. Chehovskiy, V. V. Preobrazhenskii, M. A. Putyato, and T. A. Gavrilova, Physica E **6**, 828 (2000).
[6] O. G. Schmidt and K. Eberl, Nature **410**, 168 (2001).
[7] Y. F. Mei, G. S. Huang, A. A. Solovev, E. B. Ureña, I. Mönch, F. Ding, T. Reindl, K. Y. Fu, P. K. Chu, and O. G. Schmidt, Adv. Mater. **20**, 4085 (2008).
[8] M. H. Huang, C. Boone, M. Roberts, D. E. Savage, M. G. Lagally, N. Shaji, H. Qin, R. Blick, J. A. Nairn, and F. Liu, Adv. Mater. **17**, 2860 (2005).
[9] J. X. Li, J. Zhang, W. Gao, G. S. Huang, Z. F. Di, R. Liu, J. Wang, and Y. F. Mei, Adv. Mater. **25**, 3715 (2012).
[10] A. Malachias, Ch. Deneke, B. Krause, C. Mocuta, S. Kiravittaya, T. H. Metzger, and O. G. Schmidt, Phys. Rev. B **79**, 035301 (2009).
[11] R. Songmuang, N. Y. Jin-Phillipp, S. Mendach, and O. G. Schmidt, Appl. Phys. Lett. **88**, 021913 (2006).
[12] A. Bernardi, A. R. Goñi, M. I. Alonso, F. Alsina, H. Scheel, P. O. Vaccaro, and N. Saito, J. Appl. Phys. **99**, 063512 (2006).
[13] B. Krause, C. Mocuta, T. H. Metzger, Ch. Deneke, and O. G. Schmidt, Phys. Rev. Lett. **96**, 165502 (2006).
[14] Ch. Deneke, A. Malachias, S. Kiravittaya, M. Benyoucef, T. H. Metzger, and O. G. Schmidt, Appl. Phys. Lett. **96**, 143101 (2010).
[15] H. L. Zhen, G. S. Huang, S. Kiravittaya, S. L. Li, Ch. Deneke, D. J. Thurmer, Y. F. Mei, O. G. Schmidt, and W. Lu, Appl. Phys. Lett. **102**, 041109 (2013).
[16] J. A. Rogers, M. G. Lagally, and R. G. Nuzzo, Nature **477**, 45 (2011).
[17] G. S. Huang and Y. F. Mei, Adv. Mater. **24**, 2517 (2012).
[18] J. R. Jain, A. Hryciw, T. M. Baer, D. A. B. Miller, M. L. Brongersma, and R. T. Howe, Nat. Photon. **6**, 398 (2012).
[19] M. J. Suess, R. Geiger, R. A. Minamisawa, G. Schiefler, J. Frigerio, D. Chrastina, G. Isella, R. Spolenak, J. Faist, and H. Sigg, Nat. Photon. **7**, 466 (2013).
[20] J. Welser, J. L. Hoyt, and J. F. Gibbons, IEEE Electron Dev. Lett. **15**, 100 (1994).
[21] Y. F. Mei, S. Kiravittaya, S. Harazim, and O. G. Schmidt, Mater. Sci. & Eng. R: Reports **70**, 209 (2010).
[22] J. F. Liu, X. C. Sun, D. Pan, X. X. Wang, L. C. Kimerling, T. L. Koch, and J. Michel, Opt. Exp. **15**, 11272 (2007).
[23] J. R. Sanchez-Perez, C. Boztug, F. Chen, F. F. Sudradjat, D. M. Paskiewicz, R. Jacobson, M. G. Lagally, and R. Paiella, Proc. Nat. Acad. Sci. U.S.A. **108**, 18893 (2011).
[24] M. El Kurdi, H. Bertin, E. Martincic, M. de Kersauson, G. Fishman, S. Sauvage, A. Bosseboeuf, and P. Boucaud, Appl. Phys. Lett. **96**, 041909 (2010).
[25] J. Greil, A. Lugstein, C. Zeiner, G. Strasser, and E. Bertagnolli, Nano Lett. **12**, 6230 (2012).
[26] A. Thorton and W. D. Hoffman, Thin Solid Films **171**, 5 (1989).
[27] I. S. Chun, A. Challa, B. Derickson, K. J. Hsia, and X. L. Li, Nano Lett. **10**, 3927 (2010).
[28] L. Zhang, E. Ruh, D. Grutzmacher, L. X. Dong, D. J. Bell, B. J. Nelson, and C. Schonenberger, Nano Lett. **6**, 1311 (2006).
[29] M. J. Suess, R. A. Minamisawa, R. Geiger, K. K. Bourdelle, H. Sigg, and R. Spolenak, Nano Lett. **14**, 1249 (2014).
[30] G. D. Sun, M. Zhang, Z. Y. Xue, Q. L. Guo, D. Chen, Z. Q. Mu, L. X. Dong, X. Wang, and Z. F. Di, Appl. Phys. Lett. **105**, 193505 (2014).
[31] K. Mizoguchi and S. Nakashima, J. Appl. Phys. **65**, 2583 (1989).
[32] Masashi Kurosawa, Taizoh Sadoh, and Masanobu Miyao, Appl. Phys. Lett. **98**, 012110 (2011).
[33] Z. Suo, E. Y. Ma, H. Gleskova, and S. Wagner, Appl. Phys. Lett. **74**, 1177 (1999).
[34] T. Miyatake and G. J. Pezzotti, J. Appl. Phys. **110**, 093511 (2011).